DOI: 10.1002/chem.200802019

# Highly Selective Dehydrogenative Silylation of Alkenes Catalyzed by Rhenium Complexes

**Yanfeng Jiang, Olivier Blacque, Thomas Fox, Christian M. Frech, and Heinz Berke*[a]**

**Abstract:** Rhenium(I) complexes of type $[ReBr_2(L)(NO)(PR_3)_2]$ (L = $H_2$ (**1**), $CH_3CN$ (**2**), and ethylene (**3**); R = *i*Pr (**a**) and cyclohexyl (Cy; **b**)) catalyze dehydrogenative silylation of alkenes in a highly selective manner to yield silyl alkenes and the corresponding alkanes. Hydrosilylation products appear only rarely depending on the type of olefinic substituent, and if they do appear then it is in very minor amounts. Mechanistic studies showed that two rhenium(I) hydride species of type $[ReBrH(NO)(PR_3)_2]$ (R = *i*Pr (**4a**) and Cy (**4b**)) and $[ReBr(\eta^2\text{-}CH_2{=}CHR^1)H(NO)(PR_3)_2]$ ($R^1 = p\text{-}CH_3C_6H_4$, R = *i*Pr (**5a**), Cy (**5b**); $R^1$ = H, R = *i*Pr (**5a′**), Cy (**5b′**)) are involved in the initiation pathway of the catalysis. The rate-determining steps of the catalytic cycle are the phosphine dissociation from complexes of type **5** and the reductive eliminations to form the alkane components. The catalytic cycle implies that the given rhenium systems have the ability to activate C–H and Si–H bonds through the aid of a facile redox interplay of $Re^{I}$ and $Re^{III}$ species. The molecular structures of **4b** and **5a** were established by means of X-ray diffraction studies.

**Keywords:** dehydrogenative silylation · homogeneous catalysis · hydrides · hydrosilylation · rhenium

## Introduction

Simultaneous C–H and Si–H bond activation to form Si–C bonds is a very desirable, usually transition-metal-mediated step of organosilicon chemistry.[1] Along these lines unsaturated silyl compounds can be accessed from olefins and silanes.[2] Such dehydrogenative silylations, according to Equation (1a), possess in most cases unfavorable chemoselectivities with respect to competing hydrosilylations of the olefinic component, which alternatively can be written as a dehydrogenative silylation according to Equation (1b).[3] The products of Equations (1a) and (1b) are thus related by a hypothetical transfer-hydrogenation process, which allows these processes to be compared. To create an idea of the thermodynamics of such reactions, exploratory DFT calculations were carried out. For ethylene ($R^1$ = H) the dehydrogenative silylation with triethylsilane (R′ = Et) [Eq. (1a)] has an enthalpy of reaction of $-33.1\ kcal\,mol^{-1}$ and the hydrosilylation to $-29.7\ kcal\,mol^{-1}$, thus showing a preference for the dehydrogenative silylation by $3.4\ kcal\,mol^{-1}$. A similar result was obtained for the dehydrogenative silylation of styrene ($R^1$ = Ph) and triethylsilane (R′ = Et), with energies of −28.6 ((*E*)-silylstyrene) and $-24.1\ kcal\,mol^{-1}$ ((*Z*)-silylstyrene) being obtained for the production of silyl styrene and ethyl benzene following Equation (1a). The competing hydrosilylation of styrene following Equation (1b) was also exothermic and amounted to a gain in energy of $-23.1$ kcal $mol^{-1}$, thus showing an energy difference of $5.5\ kcal\,mol^{-1}$ for both reactions in favor of the dehydrogenative silylation. The dehydrogenative silylation reaction of both types of olefins apparently profits from the concomitant hydrogenation process by generation of the more stable nonsilylated saturated component. Perhaps we can generalize even more and conclude from these calculations that dehydrogenative silylations and hydrosilylations are thermodynamically sound reactions with dehydrogenative silylations somewhat energetically favored over hydrosilylations. The thermodynamic difference between the reaction channels is however too small to be the decisive factor for the chemoselectivity in the catalytic process. We therefore expected any respective selectivity to be a matter of kinetics directed by the choice of an appropriate catalytic system.

Fairly selective dehydrogenative silylations according to Equation (1a) were achieved by catalysis of late transition-metal complexes,[4–9] such as $[M_3(CO)_{12}]$ species (M = Fe, Ru, Os),[4] cationic $[Rh(cod)_2]BF_4/PPh_3$ (cod = 1,5-cycloocta-

[a] Y. Jiang, Dr. O. Blacque, Dr. T. Fox, Dr. C. M. Frech, Prof. Dr. H. Berke
Anorganisch-Chemisches Institut
Universität Zürich
Winterthurerstrasse 190, 8037 Zürich (Switzerland)
Fax: (+) 41-1-63-568-02
E-mail: hberke@aci.uzh.ch

Supporting information for this article is available on the WWW under http://dx.doi.org/10.1002/chem.200802019.

   

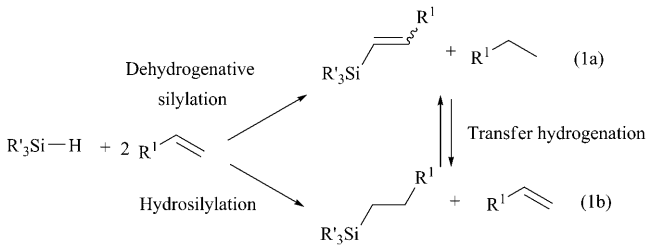


diene),[5] $[RuH_2(H_2)_2(PCy_3)_2]$ (Cy = cyclohexyl),[6] cationic $Pd^{II}$ complexes,[7] $[Ru(CO)ClH(PCy_3)_2]$,[8] and Group IV metallocenes.[10] We recently set out to explore the catalytic potential of rhenium compounds in hydrogen-based reactions and in hydrosilylations.[11] Rhenium(I) complexes of the type $[ReBr_2(L)(NO)(PR_3)_2]$ (L = $H_2$ (**1**), $CH_3CN$ (**2**), and ethylene (**3**); R = *i*Pr (**a**) and Cy (**b**)) were found to enable catalytic dehydrocoupling of $Me_2NH{\cdot}BH_3$ and transfer-hydrogenations of olefins with this reagent.[12] The same rhenium(I) complexes have now been found to catalyze dehydrogenative silylations of alkenes in a highly selective manner. Detailed mechanistic studies were carried out to shed light on the initial pathway of the reaction and the catalytic cycle.

## Results and Discussion

In an exemplary experiment, complex **1a** (1.5 mg, 1.0 mol%) was dissolved in [$D_8$]toluene (0.5 mL) containing $Et_3SiH$ (0.25 mmol) and *p*-methoxystyrene (0.50 mmol). A conversion of 95% was achieved at 100°C within 6 h. $^1$H NMR spectroscopy and GC–MS analyses indicated the formation of (*E*)-1-(*p*-methoxystyryl)-2-(triethylsilyl)-ethylene and 1-(triethylsilyl)-2-(*p*-methoxystyryl)ethane in a 19:1 ratio. *Z* isomers or branched dehydrogenative silylation products were not detected, and in contrast to other systems, addition of two equivalents of the olefin was enough to achieve high selectivities [Eq. (2)]. Complexes **1b**, **2a**,**b**, and **3a**,**b** proved to be of similar activity and selectivity (Table 1). Complexes bearing the bulky $PCy_3$ ligand are slightly more active than their $P{i}Pr_3$ derivatives, and **2a**,**b** showed somewhat lower catalytic activities (entries 6 and 7) when compared with **1a**,**b** or **3a**,**b**. Triphenylsilane ($Ph_3SiH$) is less efficient than $Et_3SiH$ (entries 10 and 11 compared with 3 and 5). Temperatures of 100°C are required in each case. Lower reaction temperatures lead to lower yields (entries 2 and 4). Other substituted styrenes, such as *p*-methyl, *p*-chloro-, and *p*-fluorostyrene also afforded the corresponding *trans*-vinylsilanes with similar yields (entries 12–14). The highest selectivity (98%) was achieved with *p*-methylstyrene. In contrast, the reaction of $Et_3SiH$ with 2-vinylnaphthalene led to a lower selectivity of 84:16 (entry 15). In the case of aliphatic alkenes a slightly higher temperature (110°C) and higher catalyst loadings were required to reach similar conversion rates. For example, the reaction of 4-allylanisole catalyzed by **1a** leads to a selectivity of 19:1 with the *E* alkene as the only product. With allyltriethoxysilane and vinylcyclohexane, dehydrogenative silylations were still preferred, but showed less *E*/*Z* selectivity (entries 19–22). Similarly, with simple alkenes such as *n*-octene the conversion was still acceptable but lower selectivity was observed (entry 16). Cyclic olefins, such as cyclooctene, gave a low conversion of 20% under the same reaction conditions. Interestingly, reactions carried out with $Et_3SiH$ and two equivalents of cyclohexyl vinyl ether yielded cyclohexyloxytriethylsilane (92%) and ethylene.[4a] Dehydrogenative silylation involving this substrate only occurred by using an

Table 1. Dehydrogenative silylation catalyzed by $Re^I$ complexes.[a]

| Entry | R′ | $R^1$ | [Re] (%) | *T* [°C] | *t* [h] | Yield[b] [%] | Dehydro(*E*/*Z*)/hydro[c] |
|---|---|---|---|---|---|---|---|
| 1 | Et | *p*-$CH_3OC_6H_4$ | – | 100 | 24 | 0 | – |
| 2 | Et | *p*-$CH_3OC_6H_4$ | **1a** (1.0) | 70 | 24 | 30 | – |
| 3 | Et | *p*-$CH_3OC_6H_4$ | **1a** (1.0) | 100 | 6 | 95 | 95(100/0):5 |
| 4 | Et | *p*-$CH_3OC_6H_4$ | **1b** (1.0) | 70 | 24 | 49 | – |
| 5 | Et | *p*-$CH_3OC_6H_4$ | **1b** (1.0) | 100 | 4 | 97 | 91(100/0):9 |
| 6 | Et | *p*-$CH_3OC_6H_4$ | **2a** (1.0) | 100 | 12 | 89 | 97(100/0):3 |
| 7 | Et | *p*-$CH_3OC_6H_4$ | **2b** (1.0) | 100 | 9 | 90 | 96(100/0):4 |
| 8 | Et | *p*-$CH_3OC_6H_4$ | **3a** (1.0) | 100 | 12 | 96 | 94(100/0):6 |
| 9 | Et | *p*-$CH_3OC_6H_4$ | **3b** (1.0) | 100 | 6 | 96 | 92(100/0):8 |
| 10[d] | Ph | *p*-$CH_3OC_6H_4$ | **1a** (1.0) | 100 | 24 | 99 | 94(100/0):6 |
| 11 | Ph | *p*-$CH_3OC_6H_4$ | **1b** (1.0) | 100 | 12 | 95 | 93(100/0):7 |
| 12 | Et | *p*-$CH_3C_6H_4$ | **1a** (1.0) | 100 | 9 | 99 | 98(100/0):2 |
| 13 | Et | *p*-$ClC_6H_4$ | **1a** (1.0) | 100 | 15 | 99 | 93(100/0):7 |
| 14 | Et | *p*-$FC_6H_4$ | **1a** (1.0) | 100 | 8 | 98 | 93(100/0):7 |
| 15 | Et | 2-naphthalenyl | **1b** (1.0) | 100 | 12 | 95 | 84(100/0):16 |
| 16 | Et | $nC_6H_{13}$ | **1a** (4.0) | 110 | 24 | 99 | 77(79/21):23 |
| 17 | Et | *p*-$CH_3OC_6H_4CH_2$ | **1a** (4.0) | 110 | 24 | 90 | 95(100/0):5 |
| 18 | Et | *p*-$CH_3OC_6H_4CH_2$ | **1b** (4.0) | 110 | 24 | 88 | 91(100/0):9 |
| 19 | Et | $(EtO)_3SiCH_2$ | **1a** (4.0) | 110 | 24 | 94 | 98(64/36):2 |
| 20 | Et | $(EtO)_3SiCH_2$ | **1b** (4.0) | 110 | 24 | 94 | 96(61/39):4 |
| 21 | Et | cyclohexyl | **1a** (4.0) | 110 | 24 | 84 | 97(56/44):3 |
| 22 | Et | cyclohexyl | **1b** (4.0) | 110 | 24 | 86 | 98(57/43):2 |
| 23[e] | Et | cyclohexyloxy | **1a** (1.0) | 110 | 7 | 79 | >99(38/62):1 |
| 24[e] | Et | cyclohexyloxy | **1b** (1.0) | 100 | 2 | 64[f] | >99(36/64):1 |
| 25[e] | Et | cyclohexyloxy | **1b** (1.0) | 100 | 10 | 82[g] | >99(37/63):1 |
| 26 | Et | H | **1a** (1.0) | 100 | 24 | 99 | 80:20 |
| 27 | Et | H | **1b** (1.0) | 100 | 24 | 99 | 79:21 |
| 28 | Et | *p*-$CH_3OC_6H_4$ | **4a** (1.0) | 100 | 5 | 99 | 98(100/0):2 |
| 29 | Et | *p*-$CH_3OC_6H_4$ | **4b** (1.0) | 100 | 3 | 99 | 98(100/0):2 |

[a] 0.25 mmol of silane and 0.50 mmol of olefin. [b] From $^1$H NMR spectroscopy integration. Hydrosilylation byproducts add up to 100%. [c] Determined by GC–MS. [d] 59% isolated yield by silicon chromatography. [e] 0.25 mmol of cyclohexyl vinyl ether with 0.375 mmol of $Et_3SiH$. [f] Traces of C–O bond-cleavage product formed. [g] Accompanied by 9% cyclohexyloxytriethylsilane.

  

excess (1.5 equiv) of $Et_3SiH$ (entries 23–25) and the *Z* product was preferably formed. In the case of ethylene, a high yield but lower dehydro/hydroselectivity (about 4:1) was observed (entries 26 and 27).

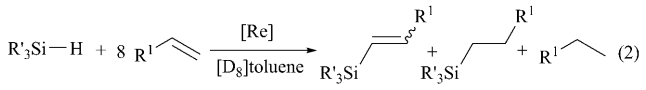


Various experiments were carried out to gain mechanistic insight. For instance, when **1b** was reacted with an excess (2–5 equiv) of $Et_3SiH$, the five-coordinate $16e^-$ rhenium(I) hydride complex $[ReBrH(NO)(PCy_3)_2]$ (**4b**) was exclusively generated. Complex **4b** was isolated in 91% yield and was fully characterized by using various spectroscopic methods. The $^1H$ NMR spectrum of **4b** exhibits a broad unresolved triplet at $\delta = -17.6$ ppm for the hydride ligand, and the $^{31}P\{^1H\}$ NMR spectrum exhibits a singlet at $\delta = 34.1$ ppm. The molecular structure of **4b** was fully established by using X-ray diffraction (Figure 1).[13] The rhenium center exhibits a square-pyramidal geometry with the hydride ligand located in an apical position, *trans* to the coordination vacancy. The two tricyclohexylphosphine ligands are arranged *trans* to each other with a P1-Re1-P2 angle of 180.0°. The *trans*-disposed π-donating bromide and π-accepting nitrosyl ligands occupy the basal sites with extra stabilization of a "push–pull" effect in an almost linear arrangement (Br1-Re1-N11 = 172.4(3)°).[14] The Re1–N11 bond length of 1.737(7) Å is in accordance with the values found in the literature[15] and the N11–O11 length of 1.221(8) Å lies in the range 1.10–1.38 Å expected for linear $NO^+$-type bonding.[15] The nitrosyl ligand is slightly bent away from linear with a Re1-N11-O11 angle of 161.8(13)°. The catalytically important stabilization of the vacant site is at least partly due to the strong *trans* influence of the hydride ligand, which leads to a weakening of any σ-type interaction at this position in such open-shell $16e^-$ rhenium(I) hydride complexes.[16] The same reaction of **1b** with $Ph_3SiH$ causes the formation of **4b**, but a large excess (100 equiv) was required, most probably due to its lower hydride donating ability when compared with $Et_3SiH$.[17] Complex **4b** was then tested as a catalyst for dehydrogenative silylation and appeared to have the same activity as **1b** (entry 29, Table 1), as anticipated when **4b** is produced along the initial catalysis pathway. Similarly, reactions of **1a** with an excess (2–5 equiv) of $Et_3SiH$ yielded the rhenium hydride complex $[ReBrH(NO)(P\mathit{i}Pr_3)_2]$ (**4a**) in 85% yield. The $^1H$ NMR spectrum of **4a** exhibits a broad signal at $\delta = -16.7$ ppm corresponding to the hydride ligand, and the $^{31}P\{^1H\}$ NMR spectrum shows a singlet at $\delta =$ 44.3 ppm. Complex **4a** has also been tested as a catalyst for the dehydrogenative silylation reaction and shows the same catalytic activity as **1a** (entry 28, Table 1).

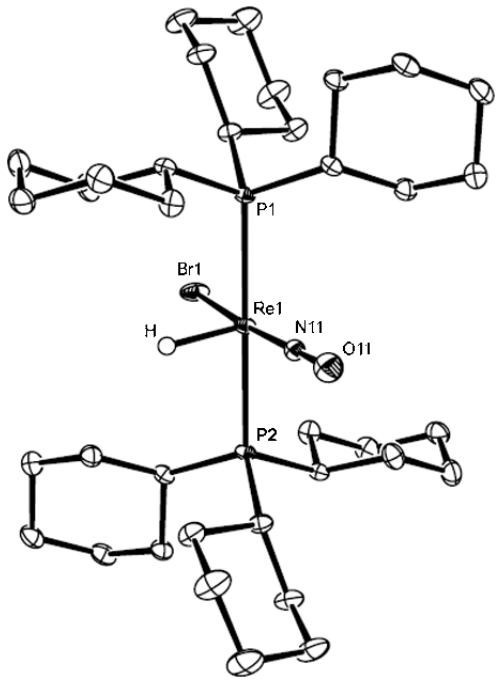


Figure 1. Molecular structure of **4b** at 30% probability ellipsoids. Selected bond lengths [Å]: Re1–H 1.55(5), Re1–N11 1.737(7), Re1–P1 2.4418(6), Re1–Br1 2.4784(7), N11–O11 1.221(8). Selected bond angles [°]: N11-Re1-Br1 172.4(3), N11-Re1-H 95.3(17), Br1-Re1-H 92.1(17), P1-Re1-H 95.8(18), P1-Re1-P2 180.0, O11-N11-Re1 161.8(13).

Reactions of **4a**,**b** with *p*-methylstyrene in toluene instantaneously and exclusively yielded their alkene adducts $[ReBr\{\eta^2\text{-}CH_2{=}CHC_6H_4(p\text{-}CH_3)\}H(NO)(PR_3)_2]$ (**5a**,**b**), which were isolated and fully characterized by using various spectroscopic methods and elemental analysis. For instance, the $^{31}P\{^1H\}$ NMR spectrum of **5b** displayed signals with AB patterns at $\delta = 2.0$ and $-0.6$ ppm ($^2J(P,P) = 122$ Hz). In addition the $^1H$ NMR spectrum exhibited a triplet signal at $\delta =$ 3.49 ppm ($^2J(H,P) = 33.3$, 36.7 Hz) corresponding to the hydride ligand. The olefinic protons of styrenes gave rise to signals at $\delta = 4.08$ (dd), 3.57 (t), and 3.32 ppm (t). In a long-range $^{13}C,^1H$ correlation spectrum (HMBC) scalar couplings between the hydride signal and the two $C_{vinyl}$ atoms ($\delta = 43.3$ and 54.1 ppm) were observed, which proved the coordination of styrene at the rhenium center. Furthermore, the scalar coupling between the $^{31}P$ NMR spectroscopy signal of one $PCy_3$ ligand at $\delta = -0.6$ ppm and the styrene vinyl proton at $\delta = 3.32$ ppm was established in a $^{31}P,^1H$ correlation spectrum ($^3J(H,P) = 7.3$ Hz), thus confirming the structure further.

The spectroscopically derived structure of **5a** was confirmed by a single-crystal X-ray diffraction study, as shown in Figure 2.[18] The coordination sphere of **5a** is pseudo-octahedral with the hydride *trans* to styrene. The bromide and nitrosyl ligands are *trans* to each other with a Br1-Re1-N1 angle of 178.84(6)°. The phosphine ligands in **5a** are markedly bent towards the H ligand with a P1-Re1-P2 angle of 145.459(17)°. Such substantial bending of phosphine molecules results not only from repulsion between the styrene and the phosphine molecules, but mainly from the optimization of $d\text{–}\pi^*_{styrene}$ orbital overlap between rhenium and styrene. Indeed, the C=C bond length (1.419(3) Å) of the Re-

  

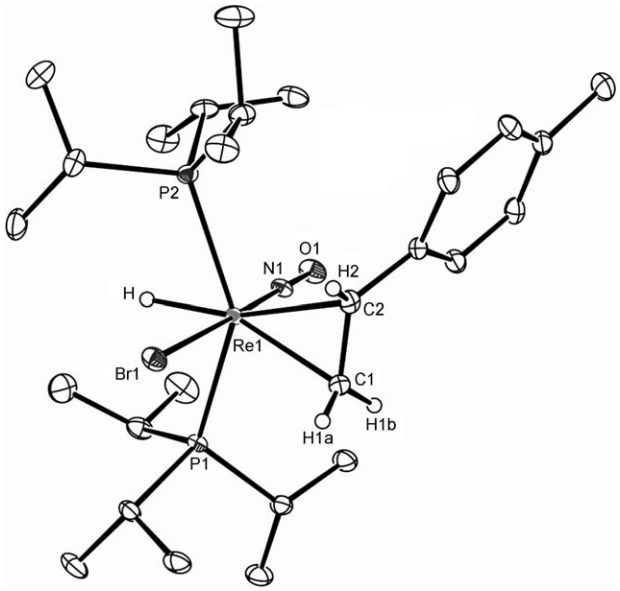


Figure 2. Molecular structure of **5a** at 30% probability ellipsoids. Selected bond lengths [Å]: C1–Re1 2.215(2), C2–Re1 2.290(2), C1–C2 1.419(3), N1–O1 1.202(2), N1–Re1 1.7429(16), P1–Re1 2.4826(5), P2–Re1 2.4970(5), Br1–Re1 2.6182(2), Re1–H 1.58(2). Selected bond angles [°]: C2-C1-Re1 74.55(12), C1-C2-Re1 68.78(12), C1-Re1-C2 36.68(8), N1-Re1-P2 95.28(5), N1-Re1-Br1 178.84(6), N1-Re1-H 95.6(7), P1-Re1-P2 145.459(17), Br1-Re1-H 83.5(7), O1-N1-Re1 178.90(15).

bound styrene in **5a** is substantially elongated compared with that in free ethylene (1.337 Å),[16,19] further stressing the strong d-electron back-donation. The $Re^{I}$-bound C=C ligand is also found in a conformation parallel to the P1-Re1-P2 axis, maximizing π back-bonding in this orientation. In this case the rhenium–alkene system could be considered as approaching the rhenium–cyclopropane extreme. In addition, the bond lengths of Re1–N1 (1.7429(16) Å), Re1–Br1 (2.6182(2) Å), and Re1–P1 (2.4826(5) Å) of **5a** are all slightly elongated relative to those in complex **4b** (Re1–N11 1.737(7) Å, Re1–Br1 2.4784(7) Å, and Re1–P1 2.4418(6) Å), and the N1–O1 bond length (1.202(2) Å) is shorter than that in **4b** (1.221(8) Å). Similarly, at room temperature the reaction of **4b** with ethylene gas immediately yielded the ethylene adduct $[ReBr(\eta^2\text{-}CH_2{=}CH_2)H(NO)(PR_3)_2]$ (**5a′**, **5b′**). Complexes **5a′** and **5b′** were fully characterized. In the $^1$H NMR spectrum, the Re–H signal of **5a′** and **5b′** are observed as triplets at $\delta = 3.75$ ($^2J(H,P) = 32.4$ Hz) and 4.11 ppm ($^2J(H,P) = 33.0$ Hz), respectively. The two types of protons in the $C_2H_4$ ligand were observed as doublets at $\delta =$ 2.73 ($^3J(H,H) = 12.0$ Hz) and 2.60 ppm ($^3J(H,H) = 12.0$ Hz) for **5a′** and at $\delta = 2.84$ ($^3J(H,H) = 9.0$ Hz) and 2.60 ppm ($^3J$-(H,H) = 9.0 Hz) for **5b′**. In the $^{31}P\{^1H\}$ NMR spectrum both phosphorus atoms are chemically equivalent and exhibit a singlet at $\delta = 15.7$ ppm for **5a′** and at $\delta = 4.6$ ppm for **5b′**.

Due to the following observations, the alkene adducts of type **5** appear to be key intermediates of the initiation pathway and resting states of the catalytic cycle: 1) complexes of type **5** were found to be the major organometallic species during catalysis using **1a**,**b** and **3a**,**b**, respectively. In addition, for **2a**,**b** as a precatalyst, a structurally related $CH_3CN$ complex is assumed to take the role of **5**; 2) Complex **5a**,**b** is as active as **4a**,**b** in dehydrogenative silylation reactions; 3) A thermally induced reversible process involving **5a**,**b** was observed. When a solution of **5b** in toluene was heated, the signal in the $^{31}P\{^1H\}$ NMR spectrum became broader, which indicates a fast dynamic process presumably originating from reversible phosphine dissociation. Complex **5b** was quantitatively recovered after cooling the sample to room temperature. Addition of P*i*Pr$_3$ (5 equiv) to the solution of **5b** in toluene and heating to 100 °C for 2 h caused $PCy_3$ to be liberated. Complex **5a** became the only remaining organometallic species in solution, as established by $^{31}P\{^1H\}$ NMR spectroscopy. An excess of $PR_3$ inhibits catalysis, but does not prevent the conversion of **4a**,**b** into **5a**,**b**, which further substantiates that reversible phosphine dissociation is involved in the catalytic cycle and may be rate determining. In addition, deuterium-labeling studies were carried out with $Et_3SiD$. Dehydrogenative silylation with *p*-methoxystyrene then yielded the saturated isotopomers *p*-$CH_3OC_6H_4CHDCH_3$ and *p*-$CH_3OC_6H_4CH_2CH_2D$ in a 1:1 ratio. No evidence was provided for deuterium incorporation into *p*-$CH_3OC_6H_4CH{=}CHSiEt_3$.

Based on these results an initiation pathway and a catalytic cycle for the dehydrogenative silylation catalyzed by $Re^{I}$ complexes **1** and **3** is proposed in Scheme 1. First the 18e$^-$ species **5** is generated via the rhenium hydride complex **4**. Thermally induced dissociation of a phosphine ligand leads to the 16e$^-$ complex **6**. DFT calculations on **5a**/**6a** revealed an enthalpy of reaction energy difference of only 14 kcal mol$^{-1}$ in favor of **5a** confirming the thermal accessibility of **6a** from **5a**. Insertion of the alkene into the Re–H bond produces the Re–alkyl species **7** and **8**, respectively. This step is most probably prompted by recoordination of

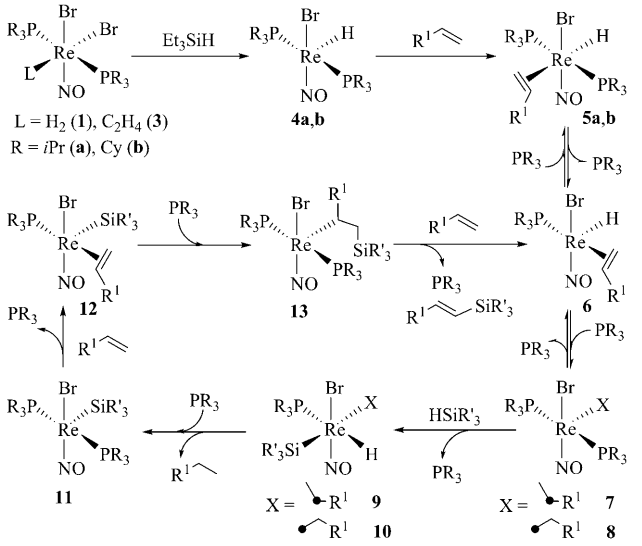


Scheme 1. Reaction initiation pathway and catalytic cycle of the dehydrogenative silylation with rhenium catalysts.

  

the phosphine ligand, which might also account for the fact that complexes bearing the more bulky $PCy_3$ ligands are more active than those with $PiPr_3$. The formation of **7** and **8** is consistent with the observation that deuterium incorporates at both the 1- and the 2-position of the vinyl group. Subsequent oxidative addition of silane to **7** or **8** leads to the $Re^{III}$ intermediate **9** or **10**, in which the Re–alkyl ligand is positioned *cis* to the less-crowded H end of the $R'_3Si{-}H$ bond rather than at the $R'_3Si$ end. At this stage the selectivity for dehydrogenative silylation is decided by preferential reductive elimination of $R^1CH_2CH_3$ to yield the Re–silyl species **11**. If a species related to **9** or **10** was formed with *cis*-$R'_3Si$ and X groups, then hydrosilylation would preferably occur by reductive elimination. Substitution of one phosphine ligand by alkene gives **12**, which undergoes insertion of alkene into the Re–silyl bond to yield **13** with the bulky silyl group attached to the less-crowded C=C end. β-Hydrogen elimination yields the dehydrogenative silylation product followed by recoordination of the alkene-generating complex **6** with closing of the catalytic cycle.[4a,20] At lower temperatures the catalytic cycle indeed terminates at the intermediate **6** to form the resting state **5**.

To gain further insight into the rate-determining steps of the catalytic cycle, deuterium isotope kinetics of the dehydrogenative silylation of *p*-methylstyrene with $Et_3SiH$ and $Et_3SiD$ catalyzed by **4b** (1.0%) were pursued at 100°C. The two curves are somewhat different in shape (Figure 3). The reaction with $Et_3SiD$ is a smooth exponential curve with a higher reaction rate in the first 60 min that reveals an inverse kinetic isotope effect ($KIE_1$) of 0.84 in this period of time. In conjunction with the observation of deuterium incorporation into the saturated product of the dehydrogenative silylation, the small $KIE_1$ value may indicate that the reductive elimination from compounds **9** or **10** (Scheme 1) contributes to the overall reaction rate. As expressed above, the predominant contribution to the overall rate is thought to originate from phosphine dissociation from complexes of type **5** or similar. Based on the inverse KIE, we assume the transition state of the reductive elimination to be late and geometrically rigid with practically fully established C–H,D bonds. Typical for such transition state cases are narrow potential-energy curves with a significantly lower-lying vibrational level for the C–D bond. In accord with the theory, we furthermore anticipate the reactant side to possess floppier bonds with softer potential-energy curves and less of an energetic difference in the vibrational levels of the bonds to H and D.[21] The eliminating Re–C and Re–H,D bonds of **9** and **10** are indeed expected to reflect this physical background.

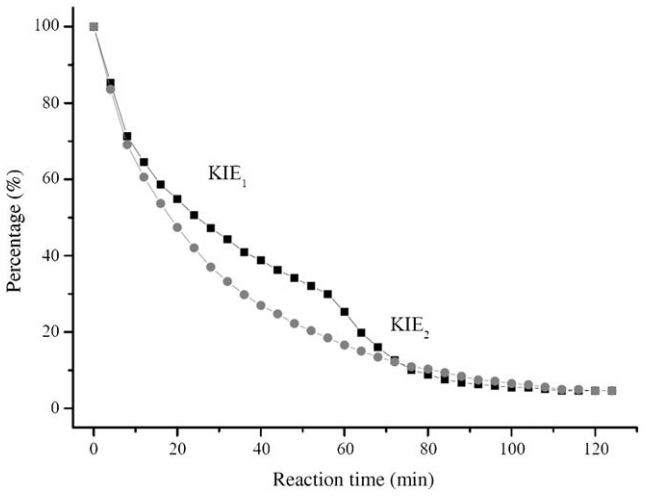


Figure 3. KIE plot of dehydrogenative silylation reaction of *p*-methylstyrene with $Et_3SiH$ (■) and $Et_3SiD$ (●) catalyzed by complex **4b** (1.0%) at 100°C. The Me resonances of $Et_3SiH$,D were monitored by using $^1H$ NMR spectroscopy ([$D_8$]toluene). An inverse $KIE_1 = 0.84$ was calculated for the range of the curves up to 60 min and in the interval of 60 to 120 min a normal $KIE_2 = 1.6$ was obtained.

Whereas the part of the curve of the reaction with $Et_3SiD$ after 60 min is expected to possess similar trends for the rates of the rate-determining steps, the comparable part of the $Et_3SiH$ curve surprisingly showed an overall rate enhancement. Apparently due to lowered concentrations of the starting materials one of the rate-determining steps switches and as a consequence a small normal kinetic isotope effect ($KIE_2$) of 1.6 is obtained. This may be interpreted in terms of the influence from the oxidative addition of the Si–H,D bonds, which possess inverse characteristics of the deuterium isotope effect in comparison with reductive eliminations. The low value of this KIE again points to phosphine dissociation as the main factor in the overall reaction rate.

The proposed reaction mechanism was supported further by the reaction of cyclohexyl vinyl ether with $Et_3SiH$. At the stage of intermediate **8**, β-O elimination occurs to give cyclohexyloxytriethylsilane and ethylene. On the other hand, oxidative addition of $Et_3SiH$ onto **8** leads to the formation of the dehydrogenative silylation product. Apparently, the latter process is only favored over the $sp^2$ C–O bond cleavage when the silane is present in excess, due to kinetic reasons.

The silyl complexes of type **11** were attempted to be prepared in various ways, however, this was met with no success. We concluded that this type of species is fairly unstable in general. One of the specific preparation routes provided evidence that the rhenium silyl species of type **11** appear only as a short-lived and unstable transient and tend to quickly react further. When the hydride **4b** was reacted with vinylsilane, silyl complexes could not be detected by using solution NMR spectroscopy. Instead, when **4b** was reacted with $Me_2PhSiCH{=}CH_2$ (2 equiv) at 100°C, the ethylene-coordinated complex $[ReBr(\eta^2\text{-}CH_2{=}CH_2)H(NO)(PCy_3)_2]$ (**5b′**) was quantitatively formed in a stoichiometric reaction accompanied by the generation of the disilyl olefins (*E*)- and (*Z*)-$Me_2PhSiCH{=}CHSiPhMe_2$ according to Scheme 2. Also in this case and in agreement with Scheme 1 the involvement of an unstable complex of type **11** is invoked as a primary product, but this then quickly decays through a "silylative coupling" channel as proposed by Wakatsuki et al.[2b] and Marciniec et al.[22]

  

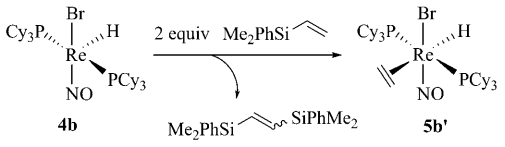


Scheme 2. Reaction of **4b** with $Me_2PhSiCH{=}CH_2$ via the formation of Re–silyl species.

## Conclusion

Rhenium(I) complexes $[ReBr_2(L)(NO)(PR_3)_2]$ (L = $H_2$ (**1**), $CH_3CN$ (**2**), and ethylene (**3**); R = *i*Pr (**a**) and Cy (**b**)) proved to be suitable catalyst precursors for the highly selective dehydrogenative silylation of alkenes to yield silylated olefins and alkanes. Hydrosilylation products were found only in rare cases, and if they were found then it was in minor amounts. The initiation stage of the catalysis involves the two types of rhenium(I) hydride species $[ReBrH(NO)(PR_3)_2]$ (**4**) and $[ReBr(\eta^2\text{-}CH_2{=}CHR^1)H(NO)(PR_3)_2]$ (**5**) and the rate-determining steps of the catalytic cycle are proposed to consist predominantly of the phosphine dissociation from complexes of type **5** and related complexes and to a minor extent also by influences of the reductive elimination of the alkanes. The catalytic cycle implies the ability of rhenium(I) complexes to activate C–H and Si–H bonds by the facile $Re^{I}$ and $Re^{III}$ redox interplay typically supported by the specific substitution patterns of the catalysts.

## Experimental Section

**General**: All manipulations were performed under an atmosphere of dry nitrogen using standard Schlenk techniques or in a glove box (M. Braun 150B-G-II) filled with dry nitrogen. Solvents were freshly distilled under $N_2$ by employing standard procedures and were degassed by freeze–thaw cycles prior to use. The deuterated solvents were dried with sodium/benzophenone ([$D_8$]toluene, [$D_6$]benzene) and vacuum transferred for storage in Schlenk flasks fitted with Teflon valves. $^1$H NMR, $^{13}C\{^1H\}$ NMR, and $^{31}P\{^1H\}$ NMR spectroscopic data were recorded on a Varian Gemini-300, a Varian Mercury 200, or a Bruker DRX 500 spectrometer using 5 mm diameter NMR tubes equipped with Teflon valves, which allow degassing and further introduction of gases into the probe. Chemical shifts are expressed in parts per million (ppm). $^1$H and $^{13}C\{^1H\}$ NMR spectra were referenced to the residual proton or $^{13}$C resonances of the deuterated solvent. All chemical shifts for the $^{31}P\{^1H\}$ NMR spectroscopy data are reported downfield in ppm relative to external 85% $H_3PO_4$ at $\delta$ = 0.0 ppm. Signal patterns are reported as follows: s, singlet; d, doublet; t, triplet; m, multiplet. IR spectra were obtained by using ATR methods with a Bio-Rad FTS-45 FTIR spectrometer. Microanalyses were carried out at the Anorganisch-Chemisches Institut of the University of Zurich. ESI-MS spectroscopic data were obtained from HCT Esquire Bruker Daltonics. $[ReBr_2(\eta^2\text{-}H_2)(NO)(P\mathit{i}Pr_3)_2]$ (**1a**), $[ReBr_2(\eta^2\text{-}H_2)(NO)(PCy_3)_2]$ (**1b**), $[ReBr_2(CH_3CN)(NO)(P\mathit{i}Pr_3)_2]$ (**2a**), $[ReBr_2(CH_3CN)(NO)(PCy_3)_2]$ (**2b**), $[ReBr_2(\eta^2\text{-}C_2H_4)(NO)(P\mathit{i}Pr_3)_2]$ (**3a**), and $[ReBr_2(\eta^2\text{-}C_2H_4)(NO)(PCy_3)_2]$ (**3b**) were prepared according to reported procedures.[11d] $Et_3SiH$, $Ph_3SiH$, alkenes, and dimethylphenylvinylsilane were purchased from Fluka and used without further purification.

**Synthesis of [ReBrH(NO)(P*i*Pr$_3$)$_2$] (4a)**: In a 50 mL Schlenk tube with a Young valve, $[ReBr_2(\eta^2\text{-}H_2)(NO)(P\mathit{i}Pr_3)_2]$ (280 mg, 0.40 mmol) and $Et_3SiH$ (144 μL, 1.0 mmol) were mixed in toluene (10 mL). After stirring at 100 °C for 3 h, the solution turned violet. The solvent was dried in vacuo. The residue was washed with cold pentane (5×3 mL) and dried again in vacuo. Yield: 210 mg, 85%. $^1$H NMR (300.1 MHz, [$D_6$]benzene): $\delta$ = 2.66 (m, 6H; P-C*H*$(CH_3)_2$), 1.29 (br, 36H; P-CH($CH_3$)$_2$), −16.7 ppm (br, 1H; Re-H); $^{13}C\{^1H\}$ NMR (75.5 MHz, [$D_6$]benzene): $\delta$ = 26.5 (br; P-*C*H$(CH_3)_2$), 21.0 (s; P-CH(*C*H$_3$)$_2$), 19.9 ppm (s; P-CH(*C*H$_3$)$_2$); $^{31}P\{^1H\}$ NMR (121.5 MHz, [$D_6$]benzene): $\delta$ = 44.3 ppm (s); IR (ATR): $\tilde{\nu}$ = 2959 (C-H), 2875 (C-H), 2093 (Re-H), 1640 cm$^{-1}$ (NO); elemental analysis calcd (%) for $C_{18}H_{43}BrNOP_2Re$ (617.60): C 35.01, H 7.02, N 2.27; found: C 34.83, H 7.02, N 2.34.

**Synthesis of [ReBrH(NO)(PCy$_3$)$_2$] (4b)**: In a 50 mL Schlenk tube with a Young valve, $[ReBr_2(\eta^2\text{-}H_2)(NO)(PCy_3)_2]$ (1.0 g, 1.0 mmol) and $Et_3SiH$ (288 μL, 2.0 mmol) were mixed in toluene (15 mL). After stirring at 100 °C for 3 h, the solution turned violet. The solvent was dried in vacuo. The residue was washed with pentane (5×3 mL) and dried again in vacuo. Yield: 781 mg, 91.0%. $^1$H NMR (300.1 MHz, [$D_8$]toluene): $\delta$ = 1.19–2.72 (m, 66H; P($C_6H_{11}$)$_3$), −17.6 ppm (t, $^2J$(H,P) = 12 Hz, 1H; Re-H); $^{13}C\{^1H\}$ NMR (75.5 MHz, [$D_8$]toluene): $\delta$ = 31.3, 30.6, 28.3, 27.1 ppm; $^{31}P\{^1H\}$ NMR (121.5 MHz, $C_6D_6$): $\delta$ = 34.1 ppm (s); IR (ATR): $\tilde{\nu}$ = 2926 (C-H), 2849 (C-H), 2098 (Re-H), 1649 cm$^{-1}$ (NO); elemental analysis calcd (%) for $C_{36}H_{67}BrNOP_2Re$ (857.98): C 50.40, H 7.87, N 1.63; found: C 50.33, H 7.68, N 1.63.

**[ReBr{η$^2$-CH$_2$=CHC$_6$H$_4$(*p*-CH$_3$)}H(NO)(P*i*Pr$_3$)$_2$] (5a)**: In a 3 mL Young NMR tube, $[ReBrH(NO)(P\mathit{i}Pr_3)_2]$ (61 mg, 0.10 mmol) and 4-methylstyrene (14 μL, 1.0 mmol) were mixed in toluene (0.5 mL). The solution turned immediately from violet to light brown. The solvent was evaporated and the residue was dissolved in hexane (2 mL). After one week light brown crystals had formed. The crystals were collected and again dried in vacuo (41 mg, 56%). $^1$H NMR (500.25 MHz, [$D_8$]toluene): $\delta$ = 7.30 (d, $^3J$(H,H) = 8 Hz, 2H; Ph), 7.07 (d, $^3J$(H,H) = 8 Hz, 2H; Ph), 4.23 (dd, $^3J$-(H,H) = 10, 15 Hz, 1H; $CH_2$=C*H*-), 3.53 (m, 1H; C$H_2$=CH-), 3.46 (t, $^3J$-(H,H) = 10 Hz, 1H; C$H_2$=CH-), 3.35 (dd, $^2J$(H,P) = 31.6, 36.3 Hz, 1H; Re-H), 2.82 (m, 3H; P-C*H*$(CH_3)_2$), 2.75 (m, 3H; P-C*H*$(CH_3)_2$), 2.18 (s, 3H; Ph-*CH*$_3$), 1.38 (m, 9H; P-CH(C*H*$_3$)$_2$), 1.24 (m, 18H; P-CH(C*H*$_3$)$_2$), 0.92 ppm (m, 9H; P-CH(C*H*$_3$)$_2$); $^{13}C\{^1H\}$ NMR (125.8 MHz, [$D_8$]toluene): $\delta$ = 146.0, 133.6, 128.7, 127.2, 54.5 (s; $CH_2$=*C*H-), 42.8 (s; *C*H$_2$=CH-), 25.7 (s; P-*C*H$(CH_3)_2$), 25.6 (s; P-*C*H$(CH_3)_2$), 25.5 (s; P-*C*H$(CH_3)_2$), 25.3 (s; P-*C*H$(CH_3)_2$), 20.9 (Ph-*CH*$_3$), 20.8 (s; P-CH(*C*H$_3$)$_2$), 20.5 (s; P-CH-(*C*H$_3$)$_2$), 19.7 (s; P-CH(*C*H$_3$)$_2$), 19.2 ppm (s; P-CH(*C*H$_3$)$_2$); $^{31}$P NMR (202.5 MHz, [$D_8$]toluene): $\delta$ = 14.2 (d, $J$ = 120 Hz, 1P), 12.6 ppm (d, $J$ = 120 Hz, 1P); IR (ATR): $\tilde{\nu}$ = 2963 (C-H), 2921 (C-H), 2874 (C-H), 2023 (Re-H), 1662 cm$^{-1}$ (NO); elemental analysis calcd (%) for $C_{27}H_{53}BrNOP_2Re$ (735.77): C 44.07, H 7.26, N 1.90; found: C 44.16, H 7.28, N 1.86.

**Synthesis of [ReBr{η$^2$-CH$_2$=CHC$_6$H$_4$(*p*-CH$_3$)}H(NO)(PCy$_3$)$_2$] (5b)**: In a 3 mL Young NMR tube, $[ReBrH(NO)(PCy_3)_2]$ (86 mg, 0.10 mmol) and *p*-methylstyrene (14 μL, 1.0 mmol) were mixed in toluene (0.5 mL). The solution immediately turned from violet to light brown. The solvent was removed in vacuo. The residue was washed with hexane (3×3 mL) and again dried in vacuo to give a light gray powder (78 mg, 80%). $^1$H NMR (500.25 MHz, [$D_8$]toluene): $\delta$ = 7.23 (d, $^3J$(H,H) = 10 Hz, 2H; Ph), 6.95 (d, $^3J$(H,H) = 10 Hz, 2H; Ph), 4.08 (dd, $^3J$(H,H) = 10, 15 Hz, 1H; $CH_2$=C*H*-), 3.55 (br, 1H; C$H_2$=CH-), 3.49 (t, $^2J$(H,P) = 33.3, 36.7 Hz, 1H; Re-H), 3.32 (t, $^3J$(H,H) = 10 Hz, 1H; C$H_2$=CH-), 2.15 (s, 3H; Ph-*CH*$_3$), 1.18–2.63 ppm (m, 66H; P($C_6H_{11}$)$_3$); $^{13}C\{^1H\}$ NMR (125.8 MHz, [$D_8$]toluene): $\delta$ = 146.2, 133.5, 129.3, 125.6, 54.2 (s; $CH_2$=*C*H-), 43.3 (s; *C*H$_2$=CH-), 36.8 (d, $J$ = 20 Hz; P-C), 35.8 (d, $J$ = 21 Hz; P-C), 32.2 (d, $J$ = 18 Hz; P-C), 31.7 (d, $J$ = 12 Hz; P-C), 30.9, 30.4, 29.6, 27.9, 27.1, 26.9, 20.9 ppm; $^{31}P\{^1H\}$ NMR (202.5 MHz, [$D_8$]toluene): $\delta$ = 1.68 (d, $J$ = 120 Hz, 1P), −1.22 ppm (d, $J$ = 120 Hz, 1P); IR (ATR): $\tilde{\nu}$ = 2920 (C-H), 2849 (C-H), 2058 (Re-H), 1670 cm$^{-1}$ (NO); elemental analysis calcd (%) for $C_{45}H_{77}BrNOP_2Re$ (975.42): C 55.37, H 7.95, N 1.43; found: C 55.55, H 8.03, N 1.38.

**Synthesis of [ReBr(η$^2$-C$_2$H$_4$)H(NO)(P*i*Pr$_3$)$_2$] (5a′)**: In a 30 mL Schlenk tube with a Young valve, $[ReBrH(NO)(P\mathit{i}Pr)_2]$ (24 mg, 0.04 mmol) was dissolved in hexane (3 mL). The nitrogen atmosphere was replaced with 1 bar of ethylene gas using a freeze–pump–thaw cycle. The mixture was stirred at room temperature for 30 min and a yellow precipitate was formed. The supernatant solution was removed and the residue was dried

  

in vacuo. Yield: 17 mg, 66%. $^1$H NMR (500.25 MHz, [D$_8$]toluene): $\delta$ = 3.75 (t, $^2J$(P,H) = 32.4 Hz, 1H; Re-H), 2.73 (d, $^2J$(H,H) = 12 Hz, 2H; $\eta^2$-C*H*H=C*H*H), 2.62 (m, 6H; P-C*H*(CH$_3$)$_2$), 2.60 (d, $^2J$(H,H) = 12 Hz, 2H; $\eta^2$-CH*H*=CH*H*), 1.20 (m, 18H; P-CH(C*H*$_3$)$_2$), 1.15 ppm (m, 18H; P-CH-(C*H*$_3$)$_2$); $^{13}$C{$^1$H} NMR (125.8 MHz, [D$_8$]toluene): $\delta$ = 34.9 (s; $\eta^2$-CH$_2$=CH$_2$), 26.0 (t, $J$(P,C) = 11.9 Hz; P-*C*H(CH$_3$)$_2$), 20.4 (s; P-CH(*C*H$_3$)$_2$), 19.6 ppm (s; P-CH(*C*H$_3$)$_2$); $^{31}$P{$^1$H} NMR (202.5 MHz, [D$_8$]toluene): $\delta$ = 15.7 ppm (s); IR (ATR): $\tilde{\nu}$ = 3005 (C-H), 2970 (C-H), 2871 (C-H), 2024 (Re-H), 1665 cm$^{-1}$ (NO); elemental analysis calcd (%) for $C_{20}H_{47}BrNOP_2Re$ (645.65): C 37.20, H 7.34, N 2.17; found: C 37.10, H 7.38, N 2.06.

**Synthesis of [ReBr($\eta^2$-C$_2$H$_4$)H(NO)(PCy$_3$)$_2$] (5b′)**: In a 50 mL Schlenk tube with a Young valve, [ReBrH(NO)(PCy$_3$)$_2$] (120 mg, 0.14 mmol) was dissolved in hexane (10 mL). The nitrogen atmosphere was replaced with ethylene gas (860 mbar) by using a freeze–pump–thaw cycle. The mixture was stirred at room temperature for 30 min and a yellow precipitate was formed. The supernatant solution was removed and the residue was dried in vacuo. Yield: 68 mg, 55%. $^1$H NMR (500.25 MHz, [D$_8$]toluene): $\delta$ = 4.11 (t, $^2J$(P,H) = 33 Hz, 1H; Re-H), 2.84 (d, $^2J$(H,H) = 9 Hz, 2H; $\eta^2$-C*H*H=C*H*H), 2.60 (d, $^2J$(H,H) = 9 Hz, 2H; $\eta^2$-CH*H*=CH*H*), 1.23–2.59 ppm (m, 66H; P(C$_6$H$_{11}$)$_3$); $^{13}$C{$^1$H} NMR (125.8 MHz, [D$_8$]toluene): $\delta$ = 36.5 (t, $J$(P,C) = 10 Hz; P-C), 34.5, 30.7, 30.0, 28.0 (m; $\eta^2$-C$_2$H$_4$), 27.1 ppm; $^{31}$P{$^1$H} NMR (202.5 MHz, [D$_8$]toluene): $\delta$ = 4.60 ppm (s); IR (ATR): $\tilde{\nu}$ = 2928 (C-H), 2851 (C-H), 2089 (Re-H), 1668 cm$^{-1}$ (NO); elemental analysis calcd (%) for $C_{38}H_{71}BrNOP_2Re$ (887.04): C 51.51, H 8.08, N 1.58; found: C 51.73, H 8.26, N 1.55.

**Catalytic dehydrogenative silylation of alkenes with R′$_3$SiH by rhenium complexes**: In a Schlenk tube with a Young valve, substrate R′$_3$SiH (0.25 mmol), an alkene (0.50 mmol), and an appropriate amount of rhenium catalyst (0.0025 or 0.01 mmol) were mixed in [D$_8$]toluene (0.5 mL). The mixture was kept stirring in the closed system at 100 or 110 °C. After an appropriate reaction time the yield and product distribution were determined by $^1$H NMR spectroscopy and GC–MS analyses.

**(*E*)-1-(*p*-Methoxystyryl)-2-(triphenylsilyl)ethylene**: A catalytic amount of **1a** (7 mg, 0.01 mmol), substrate Ph$_3$SiH (260 mg, 1.00 mmol), and 4-methoxystyrene (268 μL, 2.00 mmol) were added to a 30 mL Schlenk tube with a Young valve. The mixture was dissolved in toluene (5 mL) and kept stirring in the open system at 100 °C for 24 h. The solvent was evaporated in vacuo and the residue was subjected to chromatography on a silica gel column. Pure (*E*)-1-(*p*-methoxystyryl)-2-(triphenylsilyl)-ethylene was isolated (230 mg, 59%) as a white solid using a 1:20 Et$_2$O/pentane mixture as eluent. $^1$H NMR (300.1 MHz, [D$_6$]benzene): $\delta$ = 7.20–7.74 (m, 17H; Ph), 6.90 (d, $^3J$(H,H)$_{trans}$ = 18.9 Hz, 2H; *trans*-CH=CH), 6.70 (d, $^3J$ = 8.7 Hz, 2H), 3.23 ppm (s, 3H; Ph-OC*H*$_3$); $^{13}$C{$^1$H} NMR (75.5 MHz, C$_6$D$_6$): $\delta$ = 160.6, 149.1, 136.6, 135.3, 131.4, 129.8, 128.6, 128.3, 120.2, 114.3, 54.8 ppm; MS (ESI): *m*/*z* (%): 415.1 (100) [*M*+Na$^+$].

**Treatment of the catalytic system with excess of PR$_3$**: A catalytic amount of **4b** (2.3 mg, 0.0025 mmol), Et$_3$SiH (38 μL, 0.25 mmol), 4-methoxystyrene (67 μL, 0.50 mmol), and PCy$_3$ (7 mg, 0.025 mmol) were mixed with [D$_8$]toluene (0.5 mL) in a 30 mL Schlenk tube with a Young valve. The mixture was kept stirring at 100 °C. After 12 h, the $^1$H NMR spectrum indicated no reaction. However, the $^{31}$P NMR spectrum showed the formation of complex **5b**.

**Treatment of 1b with Ph$_3$SiH**: In a Young NMR tube, **1b** (8.4 mg, 0.01 mmol) and Ph$_3$SiH (260 mg, 1.00 mmol) were mixed in toluene (0.5 mL). The mixture was heated at 100 °C. After 12 h, the $^{31}$P NMR spectrum indicated the formation of **4b** in 76% yield.

**Phosphine dissociation study of complex 5a and 5b**: In a Young NMR tube, **1b** (8.4 mg, 0.01 mmol) and P*i*Pr$_3$ (11 μL, 0.05 mmol) were mixed in toluene (0.5 mL). The mixture was heated at 100 °C. After 1 min, the $^{31}$P NMR spectrum indicated the formation of liberated PCy$_3$ and **5a**, as well as unidentified complexes that might be those with mixed phosphine ligands. After 1 h at 100 °C, **5b** was completely transformed to **5a**, which was the only organometallic species in solution.

**KIE studies of the reaction of 4-methylstyrene with Et$_3$SiH and Et$_3$SiD catalyzed by 4b**: In a glove box, Et$_3$SiH (38 μL, 0.25 mmol) and 4-methylstyrene (68 μL, 0.50 mmol) were added into one Young NMR tube, and the same amounts of Et$_3$SiD (38 μL) and 4-methylstyrene (69 μL) were mixed in another Young NMR tube. Into a small vial, **4b** (4.4 mg, 0.002 mmol) was dissolved in [D$_8$]toluene (1.0 mL), which was added equivalently into the two Young NMR tubes. The solution was heated at 100 °C and the dehydrogenative silylation reaction process was monitored every 4 min by using $^1$H NMR spectroscopy.

**Attempt to synthesize Re–silyl species from 4b and Me$_2$PhSiCH=CH$_2$**: In a Young NMR tube, **1b** (8.4 mg, 0.01 mmol) and Me$_2$PhSiCH=CH$_2$ (1.8 μL, 0.01 mmol) were mixed in toluene (0.5 mL). It immediately led to the formation of the 18e$^-$ alkene adduct [ReBr($\eta^2$-CH$_2$=CHSiMe$_2$Ph)H(NO)(PCy$_3$)$_2$] at room temperature. The solution was heated at 100 °C for 30 min. $^1$H and $^{31}$P NMR spectra indicated the formation of the ethylene-coordinated rhenium hydride **5a′** and the dehydrogenative silylation product Me$_2$PhSiCH=CHSiPhMe$_2$ ($\delta$ = 6.35 ppm for SiC*H*=C*H*Si). The formation of this product could also be proven by GC–MS (*m*/*z* 296.5 [*M*$^+$]). After 4 h at 100 °C, [ReBr($\eta^2$-CH$_2$=CHSiMe$_2$Ph)H(NO)(PCy$_3$)$_2$] had totally disappeared and the hydride **5a′** became the only remaining organometallic species in solution, along with an increased amount of Me$_2$PhSiCH=CHSiPhMe$_2$.

**X-ray structural analyses of 4b and 5a**: The single-crystal X-ray diffraction studies of **4b** and **5a** were carried out on an Oxford Xcalibur diffractometer (4-circle kappa platform, Ruby charge-coupled device (CCD) detector, single-wavelength Enhance X-ray source with Mo$_{K\alpha}$ radiation, $\lambda$ = 0.71073 Å) at 183(2) K.[23] The crystal structures were solved with the Patterson method by applying the software options of the program SHELXS-97[24] and full-matrix least-squares refinement on $F^2$ (SHELXL-97).[24] The program PLATON[25] was used to check the result of the X-ray analyses and the program ORTEP[26] was used to give a representation of the structures. All software used to prepare material for publication are included in the WINGX software.[27] For **4b**, the metal center lies on an inversion center that led to the refinement of only one half of the molecule and caused positional disorders for the bromide, nitrosyl, and hydride ligands. Furthermore, the nitrosyl ligand had to be disordered once more, because it occupied two sites near to the position of the bromide. Consequently, the nitrogen and oxygen atoms were isotropically refined. All hydrogen positions were calculated after each cycle of refinement by using a riding model except for the hydride atom, which was located in a Fourier map and geometrically refined. For **5b**, the positions of the hydride and the ethylenic hydrogen atoms were found in the difference Fourier map and freely refined. All other hydrogen positions were calculated after each cycle of refinement by using a riding model.

CCDC-681124 (**4b**) and CCDC-699750 (**5a**) contain the supplementary crystallographic data for this paper. These data can be obtained free of charge from The Cambridge Crystallographic Data Centre via www.ccdc.cam.ac.uk/data_request/cif.

**Computational details**: The geometry optimizations were performed with the Gaussian03 program package[28] using the hybrid *m*PW1PW91 functional, which includes the modified Perdew–Wang exchange and Perdew–Wang 91 correlation, in conjunction with the Stuttgart/Dresden ECPs (SDD) basis set for the Re center and the extended 6-31+G(d,p) basis set for the remaining atoms. The nature of the optimized structures was verified by frequency calculations at the same level of theory. The relative electronic energy includes the zero-point energies calculated by using the nonimaginary frequencies.

## Acknowledgements

Support from the Swiss National Science Foundation, the European COST program, and the Funds of the University of Zurich are gratefully acknowledged.

[1] M. A. Brook, *Silicon in Organic, Organometallic and Polymer Chemistry*, Wiley, New York, **2000**.

[2] a) *Comprehensive Handbook on Hydrosilylation* (Ed.: B. Marciniec), Pergamon, Oxford, **1992**, Chapter 2; b) Y. Watatsuki, H. Ya-

  

mazaki, M. Nakano, Y. Yamamoto, *J. Chem. Soc. Chem. Commun.* **1991**, 703; c) M. Tanaka, Y. Uchimara, H. J. Lautenschlager, *J. Organomet. Chem.* **1992**, *428*, 1; d) M. Brookhart, B. E. Grant, *J. Am. Chem. Soc.* **1993**, *115*, 2151; e) Y. Maruyama, K. Yamamura, I. Nakayama, K. Yoshiuchi, F. Ozawa, *J. Am. Chem. Soc.* **1998**, *120*, 1421; f) F. Kakiuchi, K. Nogami, N. Chatani, Y. Seki, S. Murai, *Organometallics* **1993**, *12*, 4748; g) N. Furukawa, N. Kourogi, Y. Seki, F. Kakiuchi, S. Murai, *Organometallics* **1999**, *18*, 3764; h) F. Kakiuchi, A. Yamada, N. Chatani, S. Murai, N. Furukawa, Y. Seki, *Organometallics* **1999**, *18*, 2033; i) S. B. Duckett, R. N. Perutz, *Organometallics* **1992**, *11*, 90.

[3] a) B. Marciniec, *Appl. Organomet. Chem.* **2000**, *14*, 527; b) B. Marciniec, *Coord. Chem. Rev.* **2005**, *249*, 2374; c) B. Marciniec, *New J. Chem.* **1997**, *21*, 815; d) B. Marciniec, *Acc. Chem. Res.* **2007**, *40*, 943; e) B. Marciniec, B. Dudziec, I. Kownacki, *Angew. Chem.* **2006**, *118*, 8360; *Angew. Chem. Int. Ed.* **2006**, *45*, 8180.

[4] a) Y. Seki, K. Takeshita, K. Kawamoto, S. Murai, N. Sonoda, *J. Org. Chem.* **1986**, *51*, 3890; b) F. Kakiuchi, Y. Tanaka, N. Chatani, S. Murai, *J. Organomet. Chem.* **1993**, *456*, 45.

[5] R. Takeuchi, H. Yasue, *Organometallics* **1996**, *15*, 2098.

[6] a) M. L. Christ, S. Sabo-Etienne, B. Chaudret, *Organometallics* **1995**, *14*, 1082; b) S. Sabo-Etienne, B. Chaudret, *Coord. Chem. Rev.* **1998**, *178–180*, 381.

[7] a) A. M. LaPointe, F. C. Rix, M. Brookhart, *J. Am. Chem. Soc.* **1997**, *119*, 906; b) F. C. Rix, M. Brookhart, P. S. White, *J. Am. Chem. Soc.* **1996**, *118*, 2436.

[8] C. S. Yi, Z. He, D. W. Lee, *Organometallics* **2000**, *19*, 2036.

[9] For other catalysts: a) H. Maciejewski, A. Sydor, B. Marciniec, M. Kubicki, P. B. Hitchcock, *Inorg. Chim. Acta* **2006**, *359*, 2989; b) J. Cipot, M. J. Ferguson, M. Stradiotto, *Inorg. Chim. Acta* **2006**, *359*, 2780; c) D. Wechsler, A. Myers, R. McDonald, M. J. Ferguson, M. Stradiotto, *Inorg. Chem.* **2006**, *45*, 4562; d) B. Marciniec, H. Maciejewski, I. Kownacki, *J. Mol. Catal. A: Chem.* **1998**, *135*, 223; e) K. Ezbiansky, P. I. Djurovich, M. LaForest, D. J. Sinning, R. Zayes, D. H. Berry, *Organometallics* **1998**, *17*, 1455; f) F. Burgos, I. Chavez, J. M. Manriquez, M. Valderrama, *Organometallics* **2001**, *20*, 1287; g) R. Skoda-Foldes, L. Kollar, B. Heil, *J. Organomet. Chem.* **1991**, *408*, 297.

[10] a) J. Y. Corey, X. Zhu, *Organometallics* **1992**, *11*, 672; b) M. R. Kosti, R. M. Waymouth, *Organometallics* **1992**, *11*, 1095.

[11] a) A. Llamazares, H. W. Schmalle, H. Berke, *Organometallics* **2001**, *20*, 5277; b) A. Choualeb, O. Blacque, H. W. Schmalle, T. Fox, T. Hiltebrand, H. Berke, *Eur. J. Inorg. Chem.* **2007**, 5246; c) A. Choualeb, E. Maccaroni, O. Blacque, H. W. Schmalle, H. Berke, *Organometallics* **2008**, *27*, 3474; d) D. Gusev, A. Llamazares, G. Artus, H. Jacobsen, H. Berke, *Organometallics* **1999**, *18*, 75.

[12] Y. Jiang, H. Berke, *Chem. Commun.* **2007**, 3571.

[13] X-ray crystal structure data for **4b**: dark red crystals; $C_{36}H_{67}BrNOP_2Re$; $M_r = 857.96$; crystal size: $0.30 \times 0.22 \times 0.20\ mm^3$; triclinic; space group $P\bar{1}$ (no. 2); $a = 9.8326(7)$, $b = 10.2397(8)$, $c = 10.9119(7)$ Å; $\alpha = 114.257(7)$, $\beta = 108.110(6)$, $\gamma = 91.996(6)°$; $V = 935.13(14)$ Å$^3$; $Z = 1$, $\rho_{calcd} = 1.523\ Mg\,m^{-3}$; $F(000) = 438$; $\mu = 4.430\ mm^{-1}$; 22025 reflections ($2\theta_{max} = 61°$), 5686 unique ($R_{int} = 0.034$); 205 parameters; $R1$ ($I > 2(I)$) = 0.021; $wR2$(all data) = 0.054; GooF = 1.048; largest difference peak and hole: 0.611 and $-0.724\ e\,Å^{-3}$.

[14] M. A. Esteruelas, L. A. Oro, *Adv. Organomet. Chem.* **2001**, *47*, 1.

[15] B. Machura, *Coord. Chem. Rev.* **2005**, *249*, 2277, and references therein.

[16] R. H. Crabtree, *The Organometallic Chemistry of The Transition Metals*, Wiley-Interscience, New York, **2001**.

[17] H. Mayr, N. Basso, G. Hagen, *J. Am. Chem. Soc.* **1992**, *114*, 3060.

[18] X-ray crystal structure data for **5a**: pale yellow crystals; $C_{27}H_{53}BrNOP_2Re$; $M_r = 735.75$, crystal size: $0.43 \times 0.39 \times 0.21\ mm^3$; monoclinic; space group $P2_1/c$ (no. 14); $a = 12.9435(1)$, $b = 15.1503(1)$, $c = 16.3665(1)$ Å; $\beta = 105.201(1)°$; $V = 3097.15(4)$ Å$^3$; $Z = 4$; $\rho_{calcd} = 1.578\ Mg\,m^{-3}$; $F(000) = 1480$; $\mu = 5.336\ mm^{-1}$; 38198 reflections ($2\theta_{max} = 65°$), 11289 unique ($R_{int} = 0.040$); 324 parameters; $R1$ ($I > 2(I)$) = 0.022; $wR2$(all data) = 0.048; GooF = 0.973; largest difference peak and hole: 1.064 and $-0.977\ e\,Å^{-3}$.

[19] L. S. Bartell, E. A. Roth, C. Hollowel, K. Kuchitsu, J. E. Young, *J. Chem. Phys.* **1965**, *42*, 2683.

[20] A. Onopchenko, E. T. Sabourin, D. L. Beach, *J. Org. Chem.* **1983**, *48*, 5101.

[21] a) M. J. Hostetler, R. G. Bergman, *J. Am. Chem. Soc.* **1992**, *114*, 7629; b) T. I. Gountchev, T. D. Tilley, *J. Am. Chem. Soc.* **1997**, *119*, 12831; c) R. M. Bullock, B. R. Bender, Isotope Methods—Homogeneous, *Encyclopedia of Catalysis*, July **2002**, and references therein (http://www.enccat.com/).

[22] a) B. Marciniec, C. Pietraszuk, *Organometallics* **1997**, *16*, 4320; b) M. Jankowska, O. Shuvalova, N. Bespalova, M. Majchrzak, B. Marciniec, *J. Organomet. Chem.* **2005**, *690*, 4492; c) C. Pietraszuk, H. Fischer, S. Rogalski, B. Marciniec, *J. Organomet. Chem.* **2005**, *690*, 5912; d) B. D. I. Kownacki, B. Marciniec, *Angew. Chem.* **2006**, *118*, 8360; *Angew. Chem. Int. Ed*, **2006**, *45*, 8180.

[23] Oxford Diffraction Xcalibur CCD diffractometer system, CrysAlis$^{Pro}$ software (version 1.171.32), Oxford Diffraction, Abingdon, Oxfordshire, England (UK), **2007**.

[24] G. M. Sheldrick, *Acta Crystallogr. Sect. A* **2008**, *64*, 112–122.

[25] A. L. Spek, *J. Appl. Crystallogr.* **2003**, *36*, 7–13.

[26] L. J. Farrugia, *J. Appl. Crystallogr.* **1997**, *30*, 565.

[27] L. J. Farrugia, *J. Appl. Crystallogr.* **1999**, *32*, 837–838.

[28] Gaussian 03, Revision C.01, M. J. Frisch, G. W. Trucks, H. B. Schlegel, G. E. Scuseria, M. A. Robb, J. R. Cheeseman, J. A. Montgomery, Jr., T. Vreven, K. N. Kudin, J. C. Burant, J. M. Millam, S. S. Iyengar, J. Tomasi, V. Barone, B. Mennucci, M. Cossi, G. Scalmani, N. Rega, G. A. Petersson, H. Nakatsuji, M. Hada, M. Ehara, K. Toyota, R. Fukuda, J. Hasegawa, M. Ishida, T. Nakajima, Y. Honda, O. Kitao, H. Nakai, M. Klene, X. Li, J. E. Knox, H. P. Hratchian, J. B. Cross, V. Bakken, C. Adamo, J. Jaramillo, R. Gomperts, R. E. Stratmann, O. Yazyev, A. J. Austin, R. Cammi, C. Pomelli, J. W. Ochterski, P. Y. Ayala, K. Morokuma, G. A. Voth, P. Salvador, J. J. Dannenberg, V. G. Zakrzewski, S. Dapprich, A. D. Daniels, M. C. Strain, O. Farkas, D. K. Malick, A. D. Rabuck, K. Raghavachari, J. B. Foresman, J. V. Ortiz, Q. Cui, A. G. Baboul, S. Clifford, J. Cioslowski, B. B. Stefanov, G. Liu, A. Liashenko, P. Piskorz, I. Komaromi, R. L. Martin, D. J. Fox, T. Keith, M. A. Al-Laham, C. Y. Peng, A. Nanayakkara, M. Challacombe, P. M. W. Gill, B. Johnson, W. Chen, M. W. Wong, C. Gonzalez, J. A. Pople, Gaussian, Inc., Wallingford CT, **2004**.

Received: October 21, 2008
Published online: January 9, 2009

  